TITLE:

Defect energetics in ZnO: A hybrid Hartree-Fock density functional study

AUTHOR(S):

Oba, Fumiyasu; Togo, Atsushi; Tanaka, Isao; Paier, Joachim; Kresse, Georg

CITATION:

Oba, Fumiyasu ...[et al]. Defect energetics in ZnO: A hybrid Hartree-Fock density functional study. PHYSICAL REVIEW B 2008, 77(24): 245202.

ISSUE DATE:

2008-06

URL:

http://hdl.handle.net/2433/84635

RIGHT:

© 2008 The American Physical Society

京都大学学術情報リポジトリ
KURENAI 紅
Kyoto University Research Information Repository

京都大学 KYOTO UNIVERSITY
A Self-archived copy in
Kyoto University Research Information Repository
https://repository.kulib.kyoto-u.ac.jp
京都大学学術情報リポジトリ KURENAI 紅 Kyoto University Research Information Repository

PHYSICAL REVIEW B **77**, 245202 (2008)

Defect energetics in ZnO: A hybrid Hartree-Fock density functional study

Fumiyasu Oba,* Atsushi Togo, and Isao Tanaka
Department of Materials Science and Engineering, Kyoto University, Sakyo, Kyoto 606-8501, Japan

Joachim Paier and Georg Kresse
Faculty of Physics, University of Vienna and Center for Computational Materials Science, A-1090 Wien, Austria
(Received 1 April 2008; published 9 June 2008)

First-principles calculations based on hybrid Hartree-Fock density functionals provide a clear picture of the defect energetics and electronic structure in ZnO. Among the donorlike defects, the oxygen vacancy and hydrogen impurity, which are deep and shallow donors, respectively, are likely to form with a substantial concentration in *n*-type ZnO. The zinc interstitial and zinc antisite, which are both shallow donors, are energetically much less favorable. A strong preference for the oxygen vacancy and hydrogen impurity over the acceptorlike zinc vacancy is found under oxygen-poor conditions, suggesting that the oxygen vacancy contributes to nonstoichiometry and that hydrogen acts as a donor, both of which are without significant compensation by the zinc vacancy. The present results show consistency with the relevant experimental observations.

DOI: 10.1103/PhysRevB.77.245202 PACS number(s): 61.72.J−, 61.72.Bb, 71.55.Gs

I. INTRODUCTION

With outstanding versatility in electrical, optical, and chemical properties, ZnO is recognized as a key material in a wide variety of commercial applications. Renewed interest has recently emerged for its ultraviolet light emission capabilities.[1] Despite the fact that a fair amount of fundamental research was stimulated by its technological importance, the defect that is relevant to the *n*-type conductivity of undoped ZnO remains controversial. In the last decade, first-principles studies have provided insight into the defect energetics and electronic structure.[2–17] The results rather consistently indicate that the oxygen vacancy (V_O) has the lowest formation energy among the donorlike defects but forms a deep electronic state. The zinc interstitial (Zn_i) can be a shallow donor but it has high formation energy. Whereas the native defects are, thus, unlikely to be the major source of the *n*-type conductivity, the hydrogen impurity was suggested as a background shallow donor,[3,11] which is followed by an experimental support.[18–21] An optically excited metastable configuration of V_O with a shallow donor state[7] and the complex of Zn_i and the nitrogen impurity[22] were also proposed as candidates.

The theoretically derived defect energetics, however, possesses huge uncertainties due to the inaccurate description of the band structure of ZnO in using the local density functionals and the exceedingly slow energy convergence with the supercell size. Notably, the local density approximation (LDA) and generalized gradient approximation (GGA) yield significantly underestimated band gaps, i.e., 0.7–0.8 eV, compared to the experimental value of 3.44 eV.[23] Two *ad hoc* correction schemes, i.e., LDA+U and empirical *a posteriori* band-gap corrections, have been used. Unfortunately, the resultant energetics even qualitatively depends on the correction procedures. For instance, the V_O formation energy is reported to be between 0.8 and 3.7 eV, even using the same plane-wave code but different correction schemes.[7–11,14,15] The situation is largely discomforting. Hence, a concise treatment that allows for large supercells and accurate band gaps is urgently needed. Hybrid Hartree-Fock density functionals seem to offer such a solution but the yet presented calculations are limited to small supercells without finite-size corrections[16] or to an embedded cluster approach that does not describe the delocalized conduction-band states well.[17]

In this paper, we, thus, report a hybrid functional study on the defects in ZnO, which is combined with careful finite-size corrections. The results are discussed with a focus on the energetics and electronic structure of the donorlike defects.

II. COMPUTATIONAL METHODS

The calculations were performed using the plane-wave projector augmented-wave (PAW) method[24] with the Perdew-Burke-Ernzerhof (PBE) GGA functional,[25] and the PBE0,[26] and Heyd-Scuseria-Ernzerhof (HSE),[27] hybrid functionals as implemented in the VASP code.[28–30] The screening parameter in HSE was fixed at a value of 0.2 $Å^{-1}$.[27] The implementation issues and extensive tests of these hybrid functionals have been reported elsewhere.[31,32] The PAW data sets with radial cutoffs of 1.2, 1.0, and 0.6 Å for Zn, O, and H, respectively, were employed with a plane-wave cutoff energy of 300 eV, where Zn 3*d*, 4*s*, 4*p*, O 2*s*, 2*p*, and H 1*s* electrons were described as valence electrons. For the native defects, V_O, Zn_i at the octahedral and tetrahedral sites [$Zn_{i(o)}$ and $Zn_{i(t)}$], the zinc antisite (Zn_O), and the zinc vacancy (V_{Zn}), as a representative acceptorlike defect,[2,4–6,8,10,14,15,17] were considered. Regarding the hydrogen impurity, a number of different forms of shallow donors have been experimentally observed.[18–21] First-principles studies suggested the presence of several stable/metastable sites for isolated interstitial hydrogen[3,12] and its mobile nature, implying a trap by other defects.[13] Furthermore, hydrogen was predicted to occupy the substitutional oxygen site.[11] Among the forms proposed, we considered two characteristic cases: interstitial hydrogen at an energetically favorable Zn-O bond-center site along the *c* axis (H_i) [3,12] and substitutional hydrogen at the oxygen site (H_O).

For the defect calculations using the hybrid functionals, 192-atom cells and a Γ-only *k*-point sampling were em-

 ©2008 The American Physical Society

京都大学 KYOTO UNIVERSITY
A Self-archived copy in
Kyoto University Research Information Repository
https://repository.kulib.kyoto-u.ac.jp
京都大学学術情報リポジトリ KURENAI 紅 Kyoto University Research Information Repository

ployed. The large cells were chosen to minimize the errors in the finite-size corrections of formation energies, as will be mentioned later. The Γ-only sampling, however, was found to cause relatively large errors in the formation energies of V_O in the neutral and + charge states (denoted also as V_O^0 and V_O^+ hereafter, where the superscripts designate the charge states), and Zn_O in the 0–3+ charge states, i.e., 0.1–0.2 eV, owing to the selective sampling of the bottom of the defect-induced localized band with a slight dispersion. The errors were corrected using the difference between the average of the eigenvalues of the defect-induced band and the eigenvalue at the Γ point. Systematic test calculations indicate that after the corrections, the errors in the formation and transition energies are small for all the considered defects, i.e., ~0.1 and ~0.05 eV, respectively. With the lattice constants fixed at the optimized values for the perfect crystal, the internal coordinates in the defect supercells were relaxed to reduce the residual forces to less than 0.05 eV/Å. Spin polarization was taken into account for V_O^+, Zn_O^{3+}, and V_{Zn}^-, which form half-occupied localized states.

The defect formation energy was evaluated as[33]

$$E_f = E_t^d - E_t^p - \sum_i \Delta n_i \mu_i + qE_F, \tag{1}$$

where E_t^d and E_t^p denote the total energies of the supercell containing a defect with the charge q and the perfect-crystal supercell, and Δn_i is the difference in the number of constituent atoms of type i. μ_i and E_F are the atomic chemical potential and the Fermi energy, respectively. μ_{Zn} and μ_O were assumed to vary between the oxygen-poor (zinc-rich) limit [$\mu_{Zn}=\mu_{Zn(bulk)}$ and $\mu_O=1/2\mu_{O_2}+\Delta H_f$, where ΔH_f denotes the heat of formation of ZnO] and the oxygen-rich limit [$\mu_{Zn}=\mu_{Zn(bulk)}+\Delta H_f$ and $\mu_O=1/2\mu_{O_2}$]. For hydrogen, $\mu_H=1/2\mu_{H_2}$ was taken as the hydrogen-rich (oxygen-poor) limit. The calculated total energies of the Zn crystal, and the O_2 and H_2 molecules were used as the respective chemical potentials.

Errors in the defect formation energies due to the spurious electrostatic interactions in the finite-sized cells were corrected using the scheme proposed by Leslie and Gillan,[34] and by Makov and Payne.[35] It assumes that the interactions between the multipoles at the defect site, and those between the multipoles and the jellium background, lead to L^{-1}, L^{-3}, and L^{-5} dependences of the formation energies (where L is the average interdefect distance). The L^{-1} term corresponds to the Madelung energy for an array of point charges q_c in an effective medium with a static dielectric constant ϵ_0, $E_c=\alpha q_c^2/2\epsilon_0 L$, where α is the appropriate Madelung constant. This term is considered to be dominant for the charged defects in the ionic crystals.[34,35]

First, the corrections for the Madelung energies were applied to the formation energies that were calculated by using the hybrid functionals. As will be detailed later, q_c was determined on the basis of the characteristics of defect-induced electronic states instead of using the formal defect charge q. For ϵ_0, an experimental value of 8.1 (Ref. 36) was taken. The formation energies after the Madelung energy corrections were then extrapolated to the dilute (infinite cell-size) limit using L^{-3} dependences derived from systematic calculations with the GGA, which were scaled by the ratio of the GGA-estimated ϵ_0 to the experimental value. The large 192-atom cells employed in the hybrid functional calculations were confirmed to produce small errors in the extrapolation: The mean (maximum) error was estimated to be 0.02 (0.06) eV. The L^{-5} dependent contributions, which are expected to be sufficiently small for the large cells, were not considered.

The GGA calculations for the evaluation of the L^{-3} dependences were performed using seven supercells with increasing size, containing up to 784 atoms, and k-point sets corresponding to $8\times8\times6$ or denser meshes for the primitive cell. A correction for filling the conduction band or emptying the valence band[33,37] was considered.

TABLE I. Calculated fundamental properties of ZnO

	a (Å)	c (Å)	ΔH_f (eV)[a]	E_{3d} (eV)	E_g (eV)
GGA-PBE	3.286	5.299	−2.82	−4.8	0.74
PBE0	3.257	5.223	−3.03	−5.9	3.18
HSE	3.261	5.225	−3.01	−5.8	2.49
HSE(a=0.375)	3.249	5.196	−3.13	−6.4	3.43
Experiment[b]	3.242	5.188	−3.63	−7.5	3.44

[a]Errors in the binding energy of the O_2 molecule associated with the large PAW radial cutoff were corrected using the binding energy calculated with a smaller radial cutoff of 0.6 Å.
[b]References 23 and 39–41.

III. RESULTS AND DISCUSSION

The fundamental properties of ZnO that were calculated by using the hybrid functionals are summarized in Table I, alongside those with the GGA and experimental values. When compared to the GGA, the PBE0 and HSE hybrid functionals improve not only the band gap (E_g) and the Zn 3d position (E_{3d}) but also the heat of formation (ΔH_f) and the lattice constants, as recently reported for HSE.[38] However, the underestimation of E_g and the underbinding of Zn 3d still prevail. This is particularly obvious for HSE, yielding a gap of 2.49 eV. For the hybrid functionals, the optimal amount of the nonlocal Fock-exchange can be system dependent.[26] By increasing the fraction from the original value of a=0.25 to 0.375 within the formalism of HSE, E_g and E_{3d} approach the experimental values. At the same time, the lattice constants (a and c) and ΔH_f are reproduced best, which is an indispensable requirement for predicting accurate defect energies. The defect calculations were, therefore, mainly performed using HSE with the fraction of the nonlocal exchange fixed at a=0.375. HSE shows much faster convergence of the exchange energy with respect to the number of k points than PBE0 not only for metals but also for semiconductors and insulators,[32] which is advantageous in large-scale hybrid functional calculations, as performed in the present study. However, since the approach with an increased fraction of the nonlocal exchange is semiempirical, selected calculations were also performed using PBE0 to confirm the main results.

京都大学 KYOTO UNIVERSITY
A Self-archived copy in
Kyoto University Research Information Repository
https://repository.kulib.kyoto-u.ac.jp
京都大学学術情報リポジトリ KURENAI 紅 Kyoto University Research Information Repository

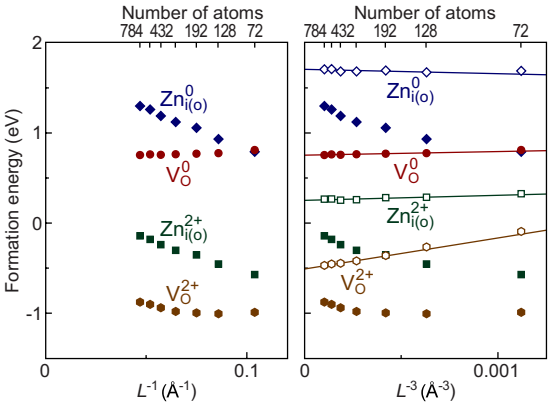

FIG. 1. (Color online) Formation energies of V_O and $Zn_{i(o)}$ in the neutral and 2+ charge states obtained by using the GGA as a function of L^{-1} and L^{-3} (where L is the average interdefect distance). The energies are for the oxygen-poor limit and the Fermi energy at the valence-band maximum. The filled and open symbols denote the values before and after the Madelung energy corrections (Refs. 34 and 35).

For the finite-size corrections of the defect formation energies, the cell-size dependence was systematically investigated by using the GGA for all the considered defects. As typical examples, the results for V_O and $Zn_{i(o)}$ in the neutral and 2+ charge states are shown in Fig. 1. For charged defects, the L^{-1} and L^{-3} dependences of the formation energies are expected on the basis of the correction model by Leslie and Gillan,[34] and by Makov and Payne.[35] After subtracting the Madelung energies (L^{-1} dependences) estimated using $q_c=q$, i.e., formal defect charge, and $\epsilon_0=9.5$, where overestimation of the electronic dielectric constant by the GGA is taken into account,[36,42] only nearly linear L^{-3} dependences are left, as illustrated for V_O^{2+} and $Zn_{i(o)}^{2+}$ in the right panel of Fig. 1. This demonstrates the appropriateness of the correction model and that the formation energies can be extrapolated to the dilute (infinite cell-size) limit using the L^{-3} dependences obtained by a linear fit.

The neutral defects show a noteworthy behavior. The formation energy of V_O^0 only slightly depends on the cell size, as expected from its neutral and localized nature. In contrast, $Zn_{i(o)}^0$ shows a strong and nearly linear L^{-1} dependence, as recognized in the left panel of Fig. 1. The slope is almost identical to that for $Zn_{i(o)}^{2+}$, indicating the presence of a Madelung energy contribution with a similar magnitude. Indeed, a Madelung energy correction for $Zn_{i(o)}^0$ using a charge of $q_c=2$ leads to a good linear L^{-3} dependence. As will be discussed later, the filling of conduction-band-like states with delocalized character, occurring also for $Zn_{i(t)}$, Zn_O, H_i, and H_O, does not effectively screen the charge of the point defect, leaving a long-range Madelung interaction between the point defects even in the neutral supercells. A similar behavior has been reported for the neutral defects in InP.[43] The proper charge q_c for the Madelung energy corrections is, therefore, approximately given by the formal defect charge plus the number of delocalized conduction-band electrons n_e, $q_c=q+n_e$, or minus the number of delocalized valence-band holes n_h, $q_c=q-n_h$. As will be shown later for the examples of V_O and Zn_i, these numbers are most easily determined by

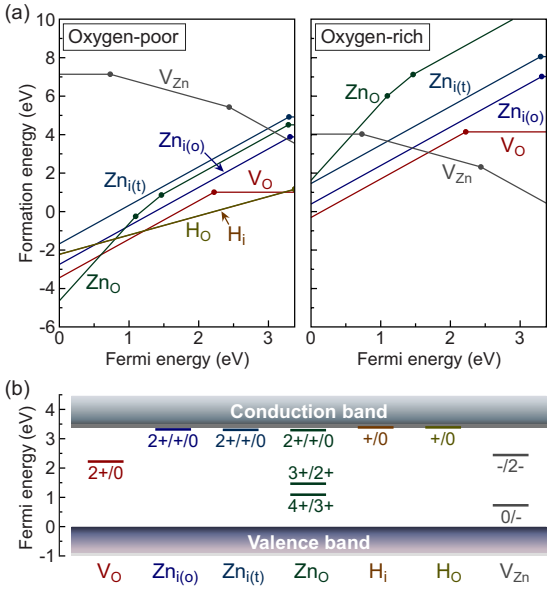

FIG. 2. (Color online) (a) Defect formation energies as a function of the Fermi energy at the oxygen-poor and oxygen-rich limits, which were obtained using the HSE(a=0.375) hybrid functional with the finite-size corrections. The slope corresponds to the charge state. (b) Defect transition levels equivalent to the filled circles in (a), alongside the relevant charge states.

inspecting the band structure: $n_e=2$ for Zn_i^0 and Zn_O^0, $n_e=1$ for Zn_i^+, Zn_O^+, H_i^0, and H_O^0, and $n_e/n_h=0$ for the rest. To accurately predict the defect formation energies and transition levels, finite-size corrections including the Madelung contributions are, thus, also required for *noncharged* defects with extended defect states. This has not been done in any of the previous studies.

Figure 2(a) presents the formation energies obtained using the HSE(a=0.375) hybrid functional with the finite-size corrections, as a function of the Fermi energy. The range of the Fermi energy is given by the calculated valence-band maximum (0 eV) and conduction-band minimum (CBM) (3.4 eV). For each geometrical defect, only the charge states that are energetically most favorable at a given Fermi energy are shown. The Fermi energies at which the slopes change correspond to the positions of thermodynamic transition levels, which are also depicted in Fig. 2(b) together with the relevant charge states.

Among the native donorlike defects, V_O shows the lowest formation energy under most conditions. Notably, the formation energy for the neutral state (V_O^0) is only 1.0 eV at the oxygen-poor limit. It exhibits a 2+/0 transition level at 1.2 eV below the CBM, confirming the previously found negative-U character, i.e., the instability of V_O^+.[2,4–10,14–16] The zinc interstitials, $Zn_{i(o)}$ and $Zn_{i(t)}$, have transition levels located at ~0.05 and ~0.1 eV below the CBM, respectively. These levels are regarded here as transition levels among the three charge states, 2+/+/0, because the 2+/+ and +/0 transition levels are different only by less than 0.05 eV, which is comparable to the accuracy of the present calculations. The possession of the 2+/+/0 transition levels near the CBM indicates that the zinc interstitials are single or double shallow donors, which is consistent with the experi-

京都大学 KYOTO UNIVERSITY
A Self-archived copy in
Kyoto University Research Information Repository
https://repository.kulib.kyoto-u.ac.jp
京都大学学術情報リポジトリ KURENAI 紅 Kyoto University Research Information Repository

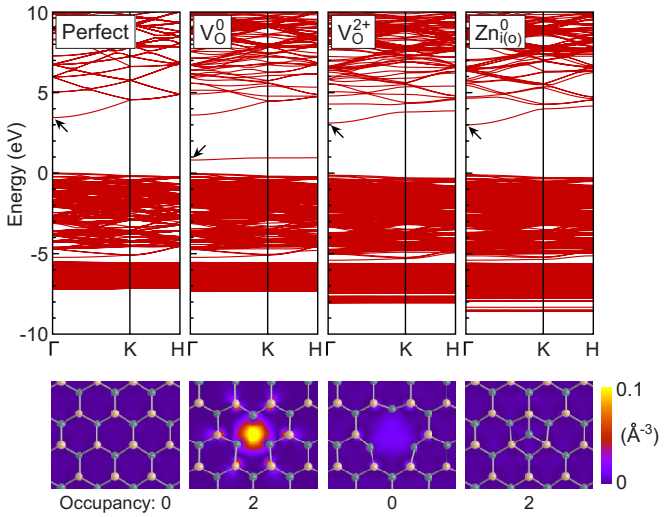

FIG. 3. (Color online) Band structure for the perfect crystal, V_O in the neutral and 2+ charge states, and $Zn_{i(o)}$ in the neutral charge state, which was obtained using the HSE(a=0.375) hybrid functional. Shown below are the squared wave functions of the states designated by the arrows, which are plotted for the middle of the (0001) Zn and O planes adjacent to the defects. The projected Zn and O atom positions are denoted with green (dark) and yellow (light) circles, respectively.

mental report (donor energy: 0.03 eV).[44] However, for the Fermi energy close to the CBM, the formation energies are as high as 4 and 5 eV even at the oxygen-poor limit. Therefore, the zinc interstitials are unlikely to form with a substantial concentration in n-type ZnO. Zn_O also has a high formation energy under n-type conditions. In addition to the shallow 2+/+/0 transition level, it shows 4+/3+ and 3+/2+ levels located below the middle of the band gap. Under oxygen-poor conditions and for a low Fermi energy, the formation energy is negative. This also holds for the other donorlike defects. A strong compensation of holes is therefore expected in ZnO grown under oxygen-poor conditions. For the hydrogen impurity, our results support its proposed role as a shallow donor.[3,11] Both H_i and H_O show +/0 transition levels nearly on the CBM and the formation energies are as low as that of V_O at the hydrogen-rich (oxygen-poor) limit.

Figure 3 shows the band structure for the 192-atom cells containing V_O^0, V_O^{2+}, and $Zn_{i(o)}^0$ that were obtained using the HSE(a=0.375) hybrid functional, alongside the band structure for the perfect crystal. For V_O^0, a localized occupied state is recognized in the band gap at 2.5–2.6 eV below the CBM. It is accompanied by a significant inward relaxation of the first-nearest-neighbor Zn ions by 10%, in stark contrast to the behavior of V_O^{2+} with an outward relaxation by 23%, and no localized states in the band gap. $Zn_{i(o)}^0$ leads only to small changes around the band gap. The highest occupied state is delocalized, which is comparable to the bottom of the conduction band in the perfect crystal. Due to this delocalized character, the removal of the electrons, i.e., changing the charge state to + or 2+, does not alter the band structure. A similar character for the defect electronic state was also found by using the GGA. The defect state of $Zn_{i(o)}^0$ is best described as a Zn^{2+} ion and two dispersed electrons located in the conduction band. If a finite-sized supercell is used to calculate the formation energy, the interaction energy between the ion and the two electrons in the conduction band is overestimated, and one can estimate the error by calculating the electrostatic interaction between +2 point charges and a homogeneous background with a total charge of −2 divided by the static dielectric constant. This is exactly the same correction usually applied for charged defects and it is easy to recognize that the combined correction is given by the Madelung energy of point charges q_c in a homogeneous background charge, where q_c is the formal defect charge plus the number of delocalized conduction-band electrons n_e, $q_c = q + n_e$. This implies that for $Zn_{i(o)}$, the same Madelung correction must be applied regardless of the formal charge state. A similar behavior in the band structure and the cell-size dependence was found for $Zn_{i(t)}$, Zn_O, H_i, and H_O.

The defect formation energies and transition levels determined in the present study not only show similarities but also important dissimilarities to the previous reports.[2–17] (i) The *thermodynamic transition level of* H_i is predicted to be located just below the CBM in all the studies. (ii) The 2+/0 *thermodynamic transition level of* V_O is estimated to be 1.2 eV below the CBM by using the present HSE(a=0.375) calculations. We obtained the same value using PBE0. An LDA+U-based approach yields 1.0 eV,[9–11] whereas the uncorrected GGA value is 0.1 eV with a large uncertainty due to the exceedingly small gap. The convergence to a single value of ~1 eV below the CBM for all methods that predict sufficiently large band gaps strongly supports the present value. This is in contrast to *a posteriori* band-gap corrections to the LDA/GGA that yield much deeper levels (e.g., 2.2 eV reported in Ref. 8). (iii) *Optical* V_O *transition levels*: A recent B3LYP hybrid functional study provided a very deep transition level for V_O, i.e., 3.0 eV below the CBM.[16] This level was determined using the one-electron energy of V_O^0 at the Γ-point, and as shown in Fig. 3, the HSE(a=0.375) one-electron energy at the Γ-point, i.e., 2.6 eV below the CBM is close to this value. The main origin of the large difference between the one-electron energies and the thermodynamic transition energies is the huge relaxation energy of 4.2 eV (Stokes shift), which happens when two electrons are removed from V_O^0 to form V_O^{2+}. In fact, the *optical transition energy* for exciting an electron from the V_O^0 defect state to the CBM ($V_O^0 \rightarrow V_O^+ + e^-$), without ionic relaxation, is determined to be 2.6 eV, which is identical to the one-electron energy. This value is in reasonable agreement with the experimental onset for the creation of paramagnetic centers (3.1 eV).[45]

Concerning the formation energies, the correction schemes for the LDA/GGA show a huge spread, as mentioned for an example of V_O in the introduction. (i) The V_O *formation energy* of 1.0 eV using HSE(a=0.375) at the oxygen-poor limit (0.9 eV using PBE0) is close to a straightforward GGA value and that with *a posteriori* band-gap corrections[8] (both 0.8 eV), whereas the LDA+U-based approach provides a much higher value (3.7 eV in Refs. 10 and 11). It is noted that our value of ~1 eV is low enough to account for the observed nonstoichiometry: e.g., 190 ppm for the specimen treated at 1373 K.[46] (ii) The *formation energies* of H_i and H_O at the hydrogen-rich limit, which are 1.2 eV or

京都大学 KYOTO UNIVERSITY
A Self-archived copy in
Kyoto University Research Information Repository
https://repository.kulib.kyoto-u.ac.jp
京都大学学術情報リポジトリ KURENAI 紅 Kyoto University Research Information Repository

lower depending on the Fermi energy, are also close to an experimental estimate of 0.8 eV,[47] again in contrast to the LDA+U-based approach yielding 2.6 and 2.7 eV, respectively.[11] (iii) Another consistency between our results and the experimental observation is found in the *relative defect energetics*: a strong preference for the donorlike defects over acceptorlike V_{Zn} under oxygen-poor conditions. This tendency is readily expected from the nonstoichiometric and n-type behavior of ZnO but has not been reproduced by the previous calculations other than applying *a posteriori* band-gap corrections to the LDA/GGA, as suggested in Refs. 4 and 8. Since V_{Zn} is not expected to exert significant effects on the composition and carrier concentration under oxygen-poor conditions, V_O (and also H_O, which can be regarded as a complex of V_O and H_i) should dominantly contribute to nonstoichiometry, and the hydrogen impurities, H_i and H_O, and/or metastable V_O with a shallow donor state[7] can effectively act as donors. The present hybrid functional approach in conjunction with careful finite-size corrections for both charged and *noncharged* supercells, thus, provides defect energetics consistent with the relevant experimental observations.

IV. CONCLUSIONS

The native defects and the hydrogen impurity in ZnO were investigated using first-principles calculations based on hybrid Hartree-Fock density functionals in conjunction with careful finite-size corrections. The results provide a clear picture of the defect energetics and electronic structure. Among the donorlike defects, V_O as a deep donor, and H_i and H_O as shallow donors, are likely to form with a substantial concentration in n-type ZnO. Zn_i and Zn_O are shallow donors but their formation is energetically much less favorable. A strong preference for V_O, H_i, and H_O over acceptorlike V_{Zn} is found under oxygen-poor conditions. It is therefore suggested that V_O (and also H_O) contributes to nonstoichiometry, and H_i and H_O act as donors, both without significant compensation by V_{Zn}. The present approach provides defect energetics in ZnO consistent with the relevant experimental observations without resorting to the empirical corrections for the valence and conduction-band positions. This constitutes a major step forward in modeling the complex behavior of semiconductors.

ACKNOWLEDGMENTS

Support by the Grant-in-Aid for Priority Area (No. 474) and Global COE Program from the MEXT, Japan, and the Austrian FWF is gratefully acknowledged.

*oba@cms.mtl.kyoto-u.ac.jp

[1] D. C. Look, B. Claflin, Y. I. Alivov, and S. J. Park, Phys. Status Solidi A **201**, 2203 (2004).
[2] A. F. Kohan, G. Ceder, D. Morgan, and Chris G. Van de Walle, Phys. Rev. B **61**, 15019 (2000).
[3] C. G. Van de Walle, Phys. Rev. Lett. **85**, 1012 (2000).
[4] S. B. Zhang, S.-H. Wei, and A. Zunger, Phys. Rev. B **63**, 075205 (2001).
[5] F. Oba, S. R. Nishitani, S. Isotani, H. Adachi, and I. Tanaka, J. Appl. Phys. **90**, 824 (2001); **90**, 3665 (2001).
[6] E.-C. Lee, Y.-S. Kim, Y.-G. Jin, and K. J. Chang, Phys. Rev. B **64**, 085120 (2001).
[7] S. Lany and A. Zunger, Phys. Rev. B **72**, 035215 (2005).
[8] S. Lany and A. Zunger, Phys. Rev. Lett. **98**, 045501 (2007).
[9] A. Janotti and C. G. Van de Walle, Appl. Phys. Lett. **87**, 122102 (2005).
[10] A. Janotti and C. G. Van de Walle, Phys. Rev. B **76**, 165202 (2007).
[11] A. Janotti and C. G. Van de Walle, Nat. Mater. **6**, 44 (2007).
[12] M. G. Wardle, J. P. Goss, and P. R. Briddon, Phys. Rev. B **72**, 155108 (2005).
[13] M. G. Wardle, J. P. Goss, and P. R. Briddon, Phys. Rev. Lett. **96**, 205504 (2006).
[14] P. Erhart, K. Albe, and A. Klein, Phys. Rev. B **73**, 205203 (2006).
[15] J.-L. Zhao, W. Zhang, X.-M. Li, J.-W. Feng, and X. Shi, J. Phys.: Condens. Matter **18**, 1495 (2006).
[16] C. H. Patterson, Phys. Rev. B **74**, 144432 (2006).
[17] A. A. Sokol, S. A. French, S. T. Bromley, C. R. A. Catlow, H. J. J. van Dam, and P. Sherwood, Faraday Discuss. **134**, 267 (2007).
[18] S. F. J. Cox *et al.*, Phys. Rev. Lett. **86**, 2601 (2001).
[19] D. M. Hofmann, A. Hofstaetter, F. Leiter, H. J. Zhou, F. Henecker, B. K. Meyer, S. B. Orlinskii, J. Schmidt, and P. G. Baranov, Phys. Rev. Lett. **88**, 045504 (2002).
[20] E. V. Lavrov, F. Borrnert, and J. Weber, Phys. Rev. B **72**, 085212 (2005).
[21] G. A. Shi, M. Stavola, S. J. Pearton, M. Thieme, E. V. Lavrov, and J. Weber, Phys. Rev. B **72**, 195211 (2005).
[22] D. C. Look, G. C. Farlow, P. Reunchan, S. Limpijumnong, S. B. Zhang, and K. Nordlund, Phys. Rev. Lett. **95**, 225502 (2005).
[23] D. C. Reynolds, D. C. Look, B. Jogai, C. W. Litton, G. Cantwell, and W. C. Harsch, Phys. Rev. B **60**, 2340 (1999).
[24] P. E. Blöchl, Phys. Rev. B **50**, 17953 (1994).
[25] J. P. Perdew, K. Burke, and M. Ernzerhof, Phys. Rev. Lett. **77**, 3865 (1996).
[26] J. P. Perdew, M. Ernzerhof, and K. Burke, J. Chem. Phys. **105**, 9982 (1996).
[27] J. Heyd, G. E. Scuseria, and M. Ernzerhof, J. Chem. Phys. **118**, 8207 (2003); **124**, 219906 (2006).
[28] G. Kresse and J. Hafner, Phys. Rev. B **48**, 13115 (1993).
[29] G. Kresse and J. Furthmüller, Phys. Rev. B **54**, 11169 (1996).
[30] G. Kresse and D. Joubert, Phys. Rev. B **59**, 1758 (1999).
[31] J. Paier, R. Hirschl, M. Marsman, and G. Kresse, J. Chem. Phys. **122**, 234102 (2005).
[32] J. Paier, M. Marsman, K. Hummer, G. Kresse, I. C. Gerber, and J. G. Ángyán, J. Chem. Phys. **124**, 154709 (2006); **125**, 249901 (2006).
[33] C. G. Van de Walle and J. Neugebauer, J. Appl. Phys. **95**, 3851 (2004).

京都大学 KYOTO UNIVERSITY
A Self-archived copy in
Kyoto University Research Information Repository
https://repository.kulib.kyoto-u.ac.jp
京都大学学術情報リポジトリ KURENAI 紅 Kyoto University Research Information Repository

[34] M. Leslie and M. J. Gillan, J. Phys. C **18**, 973 (1985).
[35] G. Makov and M. C. Payne, Phys. Rev. B **51**, 4014 (1995).
[36] N. Ashkenov *et al.*, J. Appl. Phys. **93**, 126 (2003).
[37] C. Persson, Y.-J. Zhao, S. Lany, and A. Zunger, Phys. Rev. B **72**, 035211 (2005).
[38] J. Uddin and G. E. Scuseria, Phys. Rev. B **74**, 245115 (2006).
[39] J. Albertsson, S. C. Abrahams, and A. Kvick, Acta Crystallogr., Sect. B: Struct. Sci. **45**, 34 (1989).
[40] J. D. Cox, D. D. Wagman, and V. A. Medvedev, *CODATA Key Values for Thermodynamics* (Hemisphere, New York, 1989).
[41] W. Göpel, J. Pollmann, I. Ivanov, and B. Reihl, Phys. Rev. B **26**, 3144 (1982).
[42] M. Shishkin and G. Kresse, Phys. Rev. B **75**, 235102 (2007).
[43] C. W. M. Castleton and S. Mirbt, Phys. Rev. B **70**, 195202 (2004).
[44] D. C. Look, J. W. Hemsky, and J. R. Sizelove, Phys. Rev. Lett. **82**, 2552 (1999).
[45] F. Leiter, H. Alves, D. Pfisterer, N. G. Romanov, D. M. Hofmann, and B. K. Meyer, Physica B (Amsterdam) **340-342**, 201 (2003).
[46] K. I. Hagemark and P. E. Toren, J. Electrochem. Soc. **122**, 992 (1975).
[47] J. J. Lander, J. Phys. Chem. Solids **3**, 87 (1957).